Veterinary Parasitology 339 (2025) 110588

Contents lists available at ScienceDirect

Veterinary Parasitology

journal homepage: www.elsevier.com/locate/vetpar

A novel glutathione peroxidase (EnGPX) from *Eimeria necatrix* contributes to oocyst wall biogenesis and confers protective immunity in chickens

Feiyan Wang [a,b,1], Yuemei Peng [a,b,c,1], Zhuang Ye [a,b,c], Yongcui Feng [a,b,c], Yu Zhang [a,b,c], Jinjun Xu [a,b,c], Jianping Tao [a,b,c], Dandan Liu [a,b,c,*]

[a] College of Veterinary Medicine, Yangzhou University, Yangzhou 225009, China
[b] Jiangsu Co-innovation Center for Prevention and Control of Important Animal Infectious Diseases and Zoonoses, Yangzhou University, Yangzhou 225009, China
[c] Joint International Research Laboratory of Agriculture and Agri-Product Safety, the Ministry of Education of China, Yangzhou University, Yangzhou 225009, China

ARTICLE INFO

Keywords:
Eimeria necatrix
Glutathione peroxidase
Oocyst wall
Redox regulation
Immune protection

ABSTRACT

Coccidiosis, caused by *Eimeria* spp., represents a major threat to poultry health and global food security. The oocyst wall, a crucial structure for parasite survival and transmission, is assembled through redox-dependent protein cross-linking. While glutathione peroxidases (GPXs)-mediated redox reactions play a role in oocyst wall formation, studies on GPX in *Eimeria necatrix* are limited. In this study, we identified and characterized a novel glutathione peroxidase (EnGPX) from *E. necatrix*. Bioinformatic analysis showed that EnGPX belongs to the Cys-dependent GPX (Cys-GPX) and contains a noncanonical CxxT motif within a conserved thioredoxin domain. Recombinant protein (rEnGPX) was successfully expressed, purified, and recognized by sera from *Eimeria*-infected chickens. Immunofluorescence localization revealed that EnGPX is specifically expressed in type II wall-forming bodies (WFBII) and incorporated into the oocyst wall. Transcriptional profiling showed peak EnGPX expression in unsporulated oocysts. Immunization of chickens with rEnGPX induced robust humoral responses and provided significant protection against *E. necatrix* challenge, as evidenced by reduced lesion scores, oocyst shedding, and sporulation rates. The highest dose group achieved a moderate anticoccidial index (ACI = 161.81) and a 54.85 % reduction in oocyst output, though these preliminary results require further validation through repeated experiments. Overall, our findings position EnGPX as a redox-active enzyme essential for oocyst wall biogenesis and suggest its potential as a novel subunit vaccine candidate for avian coccidiosis control.

1. Introduction

Eimeria spp. are globally enzootic parasites that cause coccidiosis in poultry, with economic losses estimated at £ 12.9 billion in 2022, partly due to the COVID-19 pandemic and ongoing regional conflicts (Blake, 2025). Currently coccidiosis control strategies rely on anticoccidial drugs, live vaccines, and environmental management. However, prolonged drug use has led to resistance and residue concerns, compromising food safety. Live vaccines are costly and show inconsistent efficacy, while environmental control in intensive systems requires substantial labor and resources (Chapman, 2018; Chapman and Rathinam, 2022; Peek and Landman, 2011). These challenges underscore the need for safe, effective and sustainable alternatives. Subunit vaccines with defined antigens represent a promising next-generation strategy (Venkatas and Adeleke, 2019).

In the life cycle of *Eimeria* spp., the oocyst is the key transmissible stage, with its multilayered wall providing environmental resilience and promoting host infection (Mai et al., 2009). The oocyst wall is assembled from gametocyte precursor proteins that are stored in wall-forming bodies (WFBs) and subsequently processed through various enzymatic modifications (Ferguson et al., 2003; Pittilo and Ball, 1980; Wang et al., 2023b). Two major classes of precursor proteins contribute to oocyst wall formation: cysteine-rich proteins involved in disulfide cross-linking, and tyrosine-rich proteins that are enzymatically cleaved into peptides undergoing redox-mediated polymerization and cross-linking, forming multi-tyrosine polymers essential for wall integrity (Mai et al., 2009). Immune-mediated disruption of oocyst wall assembly, known as immune-blocking, offers a promising vaccine strategy by

* Correspondence to: College of Veterinary Medicine, Yangzhou University, 12 East Wenhui Road, Yangzhou, Jiangsu 225009, PR China.
E-mail addresses: 243874433@qq.com (F. Wang), 2372794419@qq.com (Y. Peng), 2791744024@qq.com (Z. Ye), 1586198434@qq.com (Y. Feng), 1149027543@qq.com (Y. Zhang), jjxu@yzu.edu.cn (J. Xu), yzjptao@126.com (J. Tao), ddliu@yzu.edu.cn (D. Liu).
[1] Feiyan Wang and Yuemei Peng share first authorship

https://doi.org/10.1016/j.vetpar.2025.110588
Received 6 August 2025; Received in revised form 26 August 2025; Accepted 27 August 2025
Available online 28 August 2025

targeting a critical stage in parasite transmission (Wallach et al., 1995; Belli et al., 2003; Xu and Li, 2024).

Glutathione peroxidases (GPXs) are versatile antioxidant enzymes that catalyze the reduction of hydrogen peroxide and lipid hydroperoxides using glutathione (GSH), thereby preserving intracellular redox homeostasis (Flohé et al., 2022). Beyond their canonical role in detoxification, GPXs mediate redox-regulated protein crosslinking *via* disulfide or dityrosine bond formation-critical processes in the assembly of structural proteins (Belli et al., 2003; Brigelius-Flohé and Maiorino, 2013; Chen et al., 2016). Previous studies on *Eimeria maxima* have demonstrated that peroxidase activity is essential for the polymerization of oocyst wall proteins, highlighting the critical role of redox-mediated cross-linking in parasite development and transmission (Mai et al., 2011).

In this study, a novel GPX family member, EnGPX, was identified through differential proteomic analysis of WFBs and oocyst wall proteins in *Eimeria necatrix* (Wang et al., 2023b). The En*gpx* gene was cloned and expressed, and the localization of the encoded protein was analyzed. Immunization of broiler chickens with the recombinant protein rEnGPX significantly reduced intestinal lesions and oocyst shedding, demonstrating its potential as an immune-blocking subunit vaccine candidate against avian coccidiosis.

2. Materials and methods

2.1. Animals and parasites

The Yangzhou strain of *E. necatrix* was initially identified through both morphological examination under microscopy and molecular characterization of the internal transcribed spacer (ITS) region of the genomic DNA (Liu et al., 2014). This strain has since been maintained in the Parasitology Research Laboratory at Yangzhou University, China. Yellow-feathered chicks (One-day-old) were obtained from Jiangsu Jinghai Poultry Group Co., Ltd. and maintained in elevated wire cages in a coccidia-free environment. The birds received *ad libitum* access to antibiotic-free feed and water. Additionally, male BALB/c mice (6-weeks-old) were acquired from the Comparative Medicine Center of Yangzhou University and housed under pathogen-free conditions throughout the study period. All animal procedures were performed in accordance with the guidelines and regulations of the Animal Experiment Ethics Committee of Yangzhou University, under License No. SYXK (SU) 2022–0044 for mice and SYXK (SU) 2021–0027 for chickens.

A total of 2×10^4 sporulated oocysts of *E. necatrix* were administered orally to yellow-feathered chickens at 20 days of age. Fecal samples collected between 7 and 12 days post-infection were subjected to oocyst isolation using a saturated sodium chloride flotation technique (Liu et al., 2014). The recovered unsporulated oocysts were subsequently incubated in 2.5 % potassium dichromate at 28 °C for 72 h to induce sporulation. Second-generation merozoites (MZ-2) were isolated from the mid-intestinal epithelium at 136 h post-infection (hpi) (Su et al., 2017). Third-generation merozoites (MZ-3) and gametocytes were subsequently harvested from the mucosal tissue of the cecum at 144 and 154 hpi (Su et al., 2017; L. Wang et al., 2023b).

2.2. Cloning and sequence analysis of Engpx

Total RNA was extracted from purified gametocytes using the Fast-Pure Cell/Tissue Total RNA Isolation Kit V2 (Vazyme, Nanjing, China), following the manufacturer's protocol. Complementary DNA (cDNA) synthesis was performed using the HiScript III 1st Strand cDNA Synthesis Kit (Vazyme). Gene-specific primers were designed based on the glutathione peroxidase gene sequence of the *E. necatrix* Houghton strain (XM_013578370). RT-PCR amplification was carried out for 30 cycles under the following conditions: denaturation at 98 °C for 10 s, annealing at 55 °C for 30 s, and extension at 72 °C for 20 s. The amplified products were purified using the MiniBEST Agarose Gel DNA Extraction Kit (TaKaRa, Dalian, China), followed by A-tailing with the Mighty TA-Cloning Reagent Set for PrimeSTAR® (TaKaRa). The resulting fragments were then ligated into the pGEM®-T Easy vector (Promega, Madison, WI, USA) and subsequently sequenced by Beijing Liuhe Huada Gene Technology Co., Ltd. (Beijing, China).

Signal peptides were predicted by SignalP server (http://www.cbs.dtu.dk/services/SignalP/); Protein domains were predicted by InterPro server (http://www.ebi.ac.uk/interpro/); Protein sequences were aligned with the MegAlign (Lasergene v7.0; Madison, WI, USA), and sequence logos were generated with Weblogo 3.6 (http://weblogo.threeplusone.com/create.cgi); Protein structures were predicted, and corresponding 3D models were generated using the AlphaFold Protein Structure Database (https://alphafold.ebi.ac.uk/).

2.3. Expression and purification of recombinant protein rEnGPX

Primers were designed to introduce a 5'- Not I and a 3'- EcoR I restriction site along with protective bases into the cloned fragments, which were then ligated into the pET-28a(+) vector (Novagen, Darmstadt, Germany) to construct the recombinant plasmid pET-28a (+)-EnGPX (Table 1).

The recombinant *E. coli* strain harboring pET-28a(+)-EnGPX was inoculated into LB broth supplemented with 0.5 % glucose and cultured at 37 °C until the optical density at 600 nm (OD_{600}) reached 0.6. Protein expression was then induced by the addition of 0.2 mM IPTG, followed by incubation for an additional 5 h. The induced cells were harvested by centrifugation, washed with pre-chilled PBS, and lysed by sonication on ice (ultrasonic power: 30 W; pulse duration: 5 s; interval: 3 s). The resulting lysate was analyzed by 15 % SDS-PAGE. The recombinant protein rEnGPX was purified using nickel affinity chromatography (GenScript, Nanjing, China), renatured using a stepwise urea gradient (8 M, 6 M, 4 M and 2 M), and finally refolded by extensive dialysis against PBS.

2.4. Generation of immune sera

BALB/c mice were maintained under specific pathogen-free (SPF) conditions and immunized with rEnGPX at 6 weeks of age. The purified rEnGPX (50 μg in 50 μL of normal saline, at a concentration of 1.0 mg/mL) was rapidly mixed with 50 μL of QuickAntibody-Mouse 3 W adjuvant (Biodragon, Beijing, China). Each mouse received a 100 μL intramuscular injection of the mixture, and a booster dose was administered in the same manner one weeks later. Two weeks after the initial immunization, blood samples were collected, and sera were separated by centrifugation at 2000 × g for 10 min and stored at −80 °C for subsequent analyses.

Convalescent serum of chicken infected individually with *E. necatrix*, *E. tenella* or *E. maxima* had already been prepared and stored at −80℃ in our lab, respectively.

Table 1
Primer sequence.

Primer name	Primer sequence 5′→3′
En*gpx*-F[a]	ATGCTTCTGACGCGCGCGAC
En*gpx*-R[a]	CTACTGCAGCACACCCTCCTTG
En*gpx*-pET28aF[b]	TCGGAATTCATGCTTCTGACGCGCGCGAC
En*gpx*-pET28aR[b]	TATGCGGCCG*C*GACTGCAGCACACCCTCCTTG
En*gpx*-F[c]	TGCTTGCTGCTGACCTTTGGAG
En*gpx*-R[c]	CGTGGAACTGCTTGAGGTGCTG
5.8S rRNA-F	TTCATACTGCGTCTAATGCACC
5.8S rRNA-R	CGAGTCCTACCGCAGTACTA

Note : a, primers for complete En*gpx* gene; b, primers for prokaryotic expression; c, primers for qPCR; Restriction sites are underlined; protective bases are shown in italics.

2.5. Analysis of protein expression by western blots

The purified gametocytes were suspended in 300 μL of Pierce RIPA buffer (Thermo Fisher Scientific, Waltham, MA, USA) containing protease and phosphatase inhibitors (Xinsaimei, Shanghai, China), sonicated on ice (ultrasonic power: 30 W, pulse duration: 3 s, interval: 3 s) for 3 min. The lysate was then incubated at 4°C for 30 min and centrifuged at 10,000 × g for 10 min at 4°C. The total protein concentration in the resulting supernatants was determined using the BCA assay, after which the samples were separated by 15 % SDS-PAGE and transferred to a nitrocellulose membrane (Merck Millipore, Billerica, MA, USA). The membranes were blocked overnight at 4 °C in 3 % BSA, then incubated overnight at 4 °C in 3 % BSA with either a 6 ×His-tag monoclonal antibody (1:20,000 dilution; BIO BASIC, Markham, Canada), a mouse anti-rEnGPX pAb (1:200 dilution), or convalescent serum (1:200 dilution) from chickens individually infected with *E. necatrix*, *E. tenella*, or *E. maxima*. After incubation, the membranes were thoroughly washed with 0.03 % Tween-20 in PBS (PBST) and then incubated for 40 min at 37 °C with either horseradish peroxidase (HRP)-conjugated goat anti-mouse IgG (1:20,000 dilution; BIO BASIC) or HRP-conjugated goat anti-chicken IgY (1:20,000 dilution; BIO BASIC), respectively. Images were collected using the Tanon-5200 Chemiluminescent Imaging System (Tanon, Shanghai, China).

2.6. Indirect immunofluorescence localization of EnGPX protein

The rabbit anti-rEnGAM59 pAb was previously shown to localize EnGAM59 specifically within type II wall-forming body (WFBII) of gametocytes (Wang et al., 2023a), and thus can be used as a distinguishing marker between type I wall-forming body (WFBI). and WFBII.

Freshly isolated gametocytes and unsporulated oocysts were evenly smeared onto glass slides and fixed with methanol at −20 °C for 10 min. Following fixation, the samples were permeabilized using 0.1 % Triton X-100 (Beyotime, Shanghai, China) for 10 min at room temperature. After blocking with 3 % BSA in PBS at 37 °C for 3 h, the slides were incubated overnight at 4 °C with either anti-rEnGPX pAb (1:200 dilution) or rabbit anti-rEnGAM59 pAb (1:100 dilution; prepared in-house). Subsequently, the slides were washed three times for 15 min each with PBST (0.03 % Tween-20 in PBS), followed by incubation for 1 h at 37 °C with FITC-conjugated goat anti-mouse IgG (1:500 dilution; KPL, Gaithersburg, MD, USA) or Cy3-conjugated goat anti- rabbit IgG (1:500 dilution; KPL), as appropriate. Finally, the slides were mounted with anti-fade reagent containing DAPI (Roche, Basel, Switzerland) and examined using a fluorescence microscope (Leica DM2500, Leica Microsystems GmbH, Wetzlar, Germany).

2.7. Transcriptional analysis of Engpx in the developmental stage of E. necatrix

Total RNA was isolated from MZ-2, MZ-3 and unsporulated oocysts (UO), and subsequently reverse-transcribed into cDNA using the same protocol as that used for gametocytes. Primers were designed according to the sequences listed in Table 1, with 5.8S rRNA selected as the internal reference gene. qPCR was performed using the AceQ Universal SYBR qPCR Master Mix (Vazyme) in accordance with the manufacturer's instructions. All reactions were performed in triplicate with three independent repeats. The Ct values were recorded, and relative expression levels were calculated using the $2^{-\Delta\Delta Ct}$ method (Livak and Schmittgen, 2001). Differences were considered statistically significant at $P < 0.05$.

2.8. Immunization and challenge

In the preliminary experiment, the protective effects of rEnGPX were assessed. The experimental design and immunization schedule are shown in Table 2. Chickens with similar body weights were randomly divided into five groups (20 birds per group) on day 5. The five groups included three immunized and challenged groups (IC): rEnGPX-200 μg, rEnGPX-100 μg and rEnGPX-50 μg; and two control groups: unimmunized and challenged group (UC) and unimmunized and unchallenged group (UU). Serum samples were collected from five chickens per group on day 12 (one week after the first immunization) and day 19 (one week after the second immunization). All chickens except those in group UU, were orally challenged with 2.0×10^4 sporulated *E. necatrix* oocysts on day 19. All chickens were euthanized eight days post-challenge (day 27).

2.9. Assessment of the protective effect of rEnGPX protein

Protective efficacy was assessed using several parameters, including lesion scoring, survival percentage, relative weight gain (RWG), Oocyst reduction (OR) and the anticoccidial index (ACI) (Johnson and Reid, 1970; McManus et al., 1968). Lesions were scored on day 27 using a 0–4 scale, following the method established by Johnson and Reid (Johnson and Reid, 1970). Survival percentage was determined by calculating the proportion of live birds within each group. Body weight gain (BWG) was measured from day 19 to day 27 (BWG). RWG (%) was calculated as: (BWG of IC or UC group / BWG of UU group) × 100. OR (%) was calculated as: [(Oocyst count in UC group – Oocyst count in IC group) / Oocyst count in UC group] × 100. ACI was calculated as: [RWG (%) + Survival rate (%)] − [Oocyst value + Lesion score]. According to established criteria (McManus et al., 1968). ACI values below 120 suggest no anticoccidial activity, 120–140 indicate minimal effectiveness, 140–160 represent moderate efficacy, 160–180 indicate good efficacy, and values exceeding 180 are considered excellent.

On day 8 post-infection, unsporulated oocysts were collected from feces of each group and incubated in 2.5 % potassium dichromate at 28 °C for 72 h to induce sporulation. Sporulated and total oocysts were counted microscopically in triplicate for each group. Sporulation reduction rate (SRR, %) was calculated as: [(UC group − IC group) / UC group] × 100 %.

2.10. Serum antibody levels of chickens

Serum antibody levels were measured by indirect ELISA. Briefly, 96-well plates were coated overnight at 4 °C with 1 μg/well of purified rEnGPX. After three 15-minute washes with PBST, the wells were blocked with 3 % BSA in PBS for 1 h at 37 °C. Subsequently, serum samples (1:200 dilution) were added and incubated at 37 °C for 1 h. Plates were then washed five times with PBST, followed by incubation with HRP-conjugated goat anti-chicken IgY antibodies (1:20,000

Table 2
Details of the immunization and challenge schedule of combination of rEnGPX.

Groups	No. of chickens	Immunization dose (μg)	Immunization (d)	Immunization way	Challenge (d)	Oocysts challenge ($\times 10^4$)
rEnGPX−200 μg	10	200	5, 12	S.C	19	2.0
rEnGPX−100 μg	10	100	5, 12	S.C	19	2.0
rEnGPX−50 μg	10	50	5, 12	S.C	19	2.0
UC	10	/	/	/	19	2.0
UU	10	/	/	/	/	/

Note: S.C., subcutaneous injection

dilution; BIO BASIC). Optical density was recorded at 450 nm using a microplate reader (Sunrise-Basic, Tecan Trading AG, Männedorf, Switzerland). All assays were performed in triplicate.

2.11. Statistical analysis

Statistical analyses were performed using SPSS Statistical Software (version 26; IBM Corp., Armonk, NY, USA). Prior to inferential testing, the assumptions of normality and homogeneity of variance were assessed using the Shapiro–Wilk test and Levene's test, respectively. For

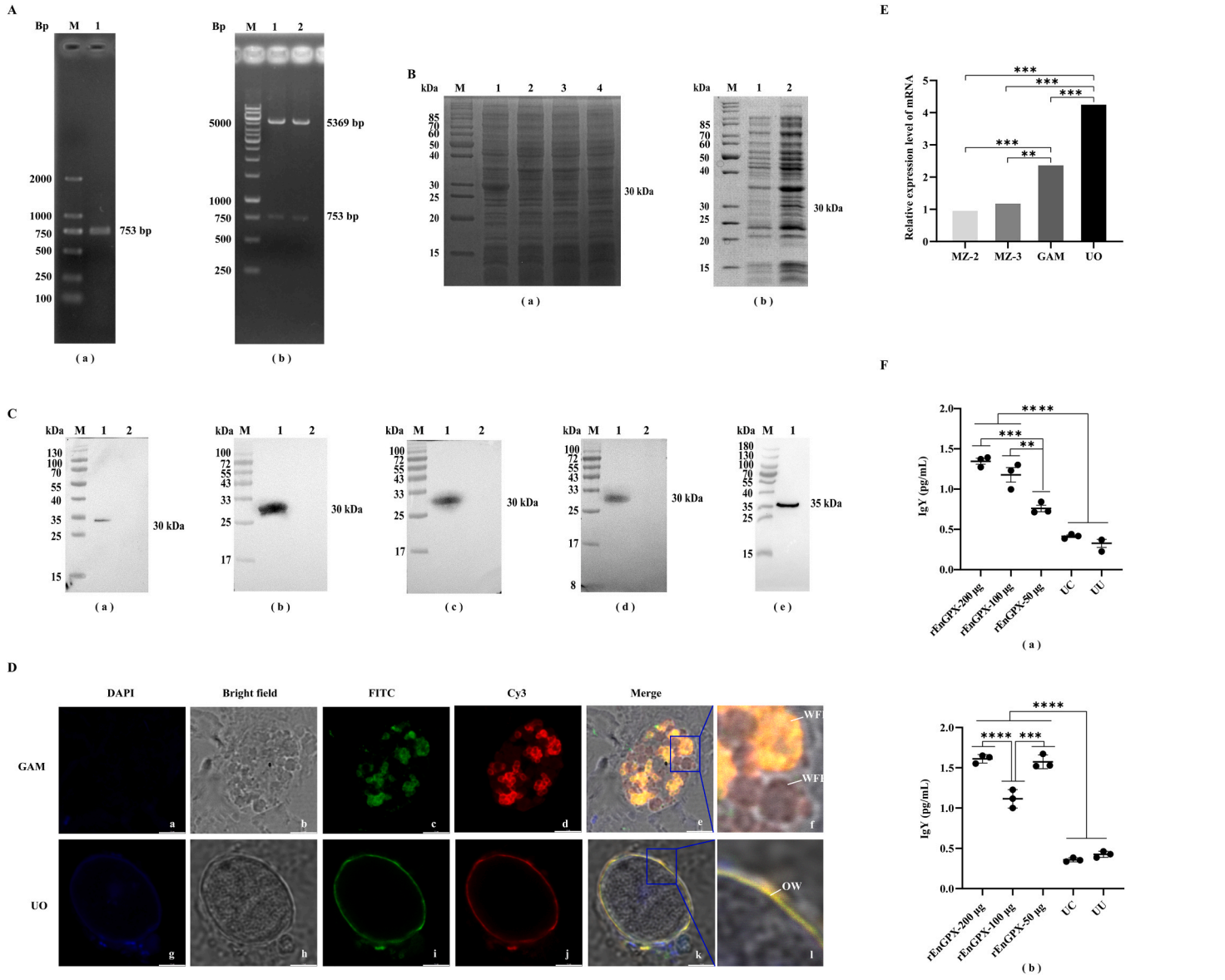

Fig. 1. (A), Gene cloning and vector construction. (a): RT-PCR amplification of En*gpx*. M: DL2 000 DNA Marker; Lane 1: En*gpx* gene RT-PCR amplification products. (b): Enzyme digestion identification of pET-28a(+)-EnGPX. M: 1 kb DNA Marker. Lane 1, 2: enzyme digestion identification of pET-28a(+)-EnGPX. (B), Expression and solubility analysis of rEnGPX protein. (a): Expression of rEnGPX protein. Lane M: unstained protein marker; Lane 1: Recombinant bacteria induced products; Lane 2: pET28a(+)-EnGPX/BL21 with IPTG induction; Lane 3: pET28a(+)-EnGPX/BL21 without IPTG induction; Lane 4: pET28a(+)/BL21 with IPTG induction. (b): Soluble analysis of rEnGPX protein: Lane M: unstained protein marker; Lane 1: Supernatant of pET28a(+)-EnGPX/BL21 with IPTG induction; Lane 2: Sediments of pET28a(+)-EnGPX/BL21 with IPTG induction. (C), Western blot analysis of rEnGPX and native protein EnGPX. The primary antibody was anti-6 ×His monoclonal antibody (a), convalescent serum of chicken infected individually with *E. necatrix* (b), *E. tenella* (c) or *E. maxima* (d). Lane M: Prestained molecular marker; Lane 1: Recombinant bacteria induced products, Lane 2: Recombinant bacteria uninduced products. (e): Western blot analysis of native protein EnGPX. Lane M: Prestained molecular marker; Lane 1: Native proteins extracted from gametocyte. (D), Localization of EnGPX in gametocytes (GAM) and unsporulated oocysts (UO) with mouse anti-rEnGPX pAb. a, g: Counter-stained with DAPI; b, h: Bright-field microscopy photographs; c, i: Immunofluorescence localization with FITC-conjuncted mouse anti-rEnGPX pAb; d, j: Immunofluorescence localization with Cy3-conjuncted Rabbit anti-rEnGAM59 pAb; e, k: The superposition of different fluorescences (Merge of images). Scale bar= 5.0 μm. f: Local enlarged drawing of e; l: Local enlarged drawing of k. (E), The transcriptional level of En*gpx* in different developmental stages. MZ-2: Second-generation of merozoites; MZ-3: Third-generation of merozoites; GAM: gametocyte; UO: Unsporulated oocysts. *Significant difference ($P < 0.05$); **significant difference ($P < 0.01$); ***significant difference ($P < 0.001$). (F), The antibody levels were measured using an indirect ELISA. Immunization with 200, 100, and 50 μg of rEnGPX resulted in significantly higher antibody levels after both the first and second immunizations compared to the UC and UU groups. The rEnGPX-200 group exhibited the highest antibody levels. Each bar represents the mean ± SD. value (n = 5) according to the Dunnett's multiple comparison tests *: significant difference ($P < 0.05$); **significant difference ($P < 0.01$); ***significant difference ($P < 0.001$); ****significant difference ($P < 0.0001$).

variables that satisfied these assumptions, one-way analysis of variance (ANOVA) was conducted, followed by Duncan's multiple range test (DMRT) for pairwise comparisons to control for type I error associated with multiple testing. All quantitative data are expressed as mean ± standard error of the mean (SEM). A p-value < 0.05 was considered statistically significant.

Oocyst count data were presented descriptively and compared visually across groups without formal significance testing, due to their highly skewed distribution and discrete nature.

3. Results

3.1. Bioinformatic analyses of EnGPX and homologous proteins

The full-length En*gpx* gene (MW588202.1) spans 753 bp (Fig. 1 A (a)), encoding a 250-amino acid protein with a predicted molecular weight of 27.7 kDa and an isoelectric point (PI) of 9.46. No signal peptide was predicted in the protein sequence.

Amino acid sequences of annotated glutathione/thioredoxin peroxidases from Apicomplexan species were aligned (Fig. 2), and a sequence logo was subsequently generated (Fig. 3). Identity analysis revealed that EnGPX (UGL75379.1) shared 99.2 % identity with the *E. necatrix* Houtong strain (XP_013436670.1) and 96.4 % identity with EtGPX from *Eimeria tenella* (XP_013231991.1). Multiple conserved regions were identified through sequence alignment, including a short CxxT motif located within the thioredoxin domain. Notably, a conserved cysteine residue at position 23 aligned with Cys108 in EnGPX, suggesting functional conservation within this motif (Fig. 3). Domain analysis further revealed that all proteins were functionally annotated as members of the thioredoxin superfamily. EnGPX and EtGPX contained thioredoxin domains spanning residues 70–235 and 69–234, respectively. The 3D structural model of EnGPX revealed a compact globular core composed of eight α-helices and eight β-strands, with a clearly extended intrinsically disordered tail. Within the core, the α-helices and β-strands intertwine to form a stable structural scaffold known as the "thioredoxin fold", which features a central four-stranded mixed β-sheet surrounded by α-helices. Cys108 is positioned at the interface between the third β-strand and the fourth α-helix, with its side chain exposed on the protein surface and surrounded by adjacent helices and strands (Fig. 4). Sequence alignment revealed that this residue is highly conserved and was predicted to serve as a potential catalytic site.

3.2. Construction of prokaryotic expression vector and expression of rEnGPX

The recombinant plasmid, designated pET-28a(+)-EnGPX, was successfully constructed and verified by double digestion with *Not* I and *Eco*R I (Fig. 1A(b)). The recombinant protein rEnGPX exhibited an approximate molecular weight of ~30 kDa (Fig. 1B(a)) and was predominantly localized in the form of inclusion bodies (Fig. 1B(b)). Purification was achieved *via* Ni-NTA affinity chromatography, yielding a distinct protein band corresponding to the target protein.

3.3. Immunoblotting analysis

Western blot analysis revealed that rEnGPX was specifically recognized by the anti-6 ×His monoclonal antibody, the mouse anti-rEnGPX pAb (Fig. 1C(a)), and convalescent sera collected from chickens of chicken infected individually with *E. necatrix* (Fig. 1C(b)), *E. tenella* (Fig. 1C(c)), and *E. maxima* (Fig. 1C(d)), each producing a distinct band of approximately 30 kDa.

Furthermore, the mouse anti-rEnGPX pAb also recognized the native gametocyte protein, which appeared as a ~35 kDa band, slightly larger than the recombinant form expressed in *E. coli* (Fig. 1C(e)).

3.4. Immunofluorescence localization

Immunofluorescence assay (IFA) results showed that the EnGPX is localized to the WFBs of gametocytes and to the oocyst wall. In contrast, no signal was detected in second- and third-generation schizonts (images not shown). Our previous research demonstrated that EnGAM59 is primarily localized to the WFBII. Co-localization analysis using rabbit anti-rEnGAM59 pAb revealed that, similar to EnGAM59, the EnGPX is predominantly distributed on WFBII within gametocytes and subsequently integrates into the oocyst wall during parasite development (Fig. 1D).

3.5. Transcription levels of Engpx

qPCR analysis (Fig. 1E) revealed that En*gpx* transcript levels were relatively low in MZ-2 and MZ-3, increased in gametocytes and UO, and reached their peak in UO, where they were significantly higher than at the other three stages ($P < 0.001$).

3.6. Protective efficacy of vaccination on E. necatrix challenge

All chickens in each group survived throughout the experiment, resulting in a 100 % survival rate. Lesion scores in all IC groups were lower than those in the UC groups, with the rEnGPX-200 μg group showing the lowest score (1.30 ± 0.23), which was significantly reduced compared to the UC group ($P < 0.05$). During the challenge phase, all IC groups exhibited higher average body weight gain than the UC group. The rEnGPX-200 μg group demonstrated the greatest weight gain (137.17 ± 7.03 g), corresponding to a relative weight gain of 94.81 %, which was significantly higher than that of the UC group.

In terms of oocyst shedding, all IC groups showed reduced oocyst output relative to the UC group. Notably, the rEnGPX-100 μg group exhibited the greatest reduction, with a 54.85 % decrease compared to the UC group. ACI analysis indicated that the rEnGPX-200 μg group achieved the highest ACI value (161.81), reflecting moderate protective

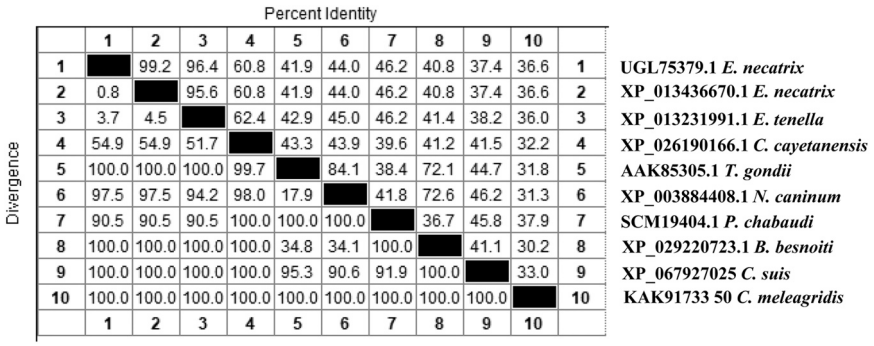

Fig. 2. A comparative amino acid sequence alignment of GPX proteins from selected Apicomplexan species was performed using ClustalW.

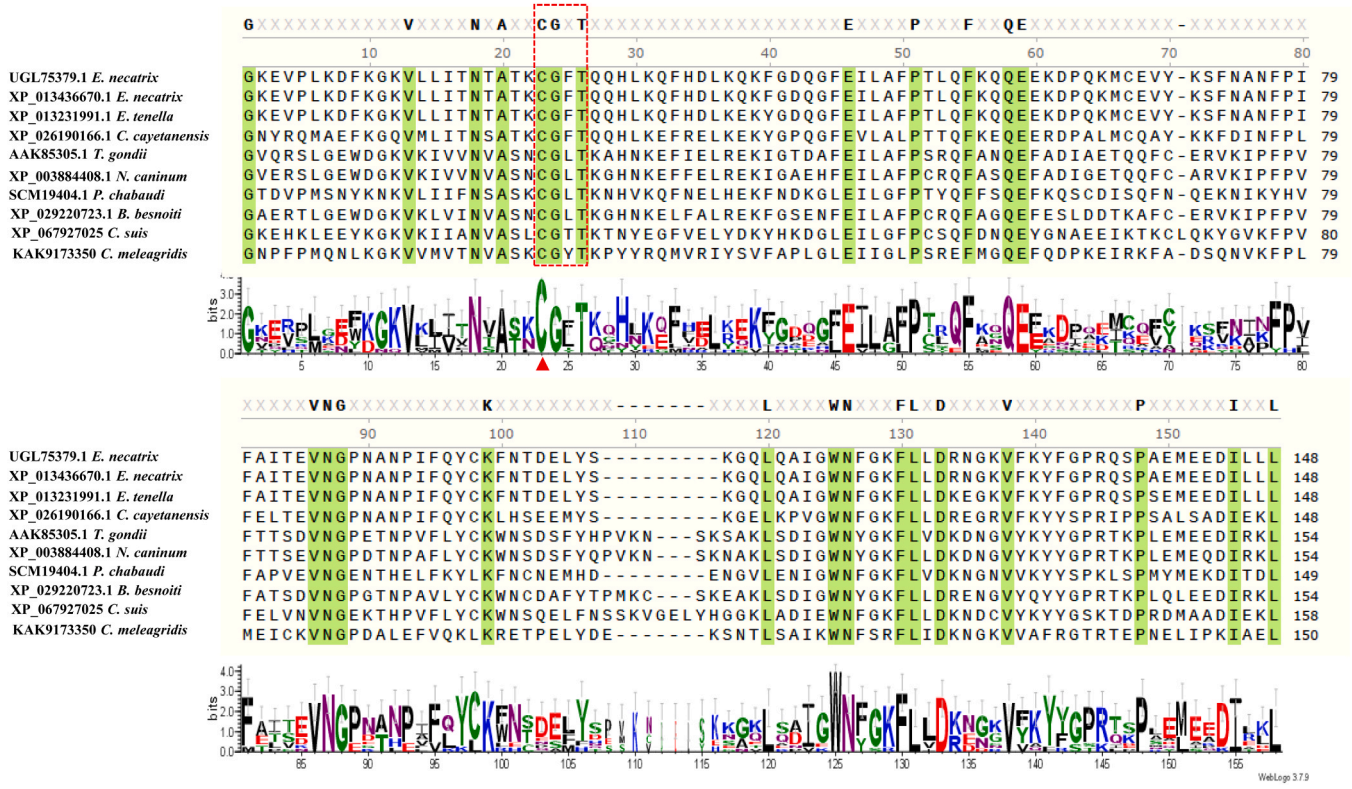

Fig. 3. Sequence logo representing the conserved amino acid residues of GPX proteins from selected Apicomplexan species. The multiple sequence alignment was generated using ClustalW, and the sequence logo was created using WebLogo (version 3.7.9). The sequences displayed, ranging from the first to the last > 95 % conserved amino acid sequences, correspond to the alignment used to generate the protein logo plot, which illustrates both the conservation and variability of the protein. The height of each letter corresponds to the relative frequency of the amino acid at that position in the aligned sequences, while the overall column height reflects the information content in bits. Highly conserved regions, such as the cysteine at position 23 (Cys108 in EnGPX, marked with a red triangle), as well as the regions spanning positions 1, 13–26, 46–59, 86–99, and 120–158 in the aligned sequences, are highlighted in green. The conserved CxxT motif is enclosed within a dashed red box.

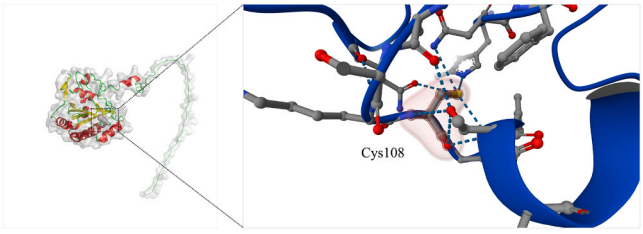

Fig. 4. The 3D structures of EnGPX protein. Overall ribbon representation of the GPX protein showing α-helices (red), β-strands (yellow), and loops (green), overlaid with a semi-transparent molecular surface. The boxed region indicates the predicted active site. The image on the right zooms is the conserved residues (Cys108) in the active site of EnGPX.

efficacy. This was followed by the rEnGPX-100 μg (157.47) and rEnGPX-50 μg (135.68) groups, the latter of which showed low protective efficacy. Although promising, these findings are preliminary and require further validation to confirm their reliability and reproducibility.

In addition, the sporulation rates of oocysts were lower in all IC groups compared to the UC group. The rEnGPX-200 μg group had the lowest sporulation rate (82.7 %), followed by the rEnGPX-100 μg (84.0 %) and rEnGPX-50 μg (87.3 %) groups (Table 3).

3.7. Serum antibody levels against rEnGPX

Serum IgY levels were evaluated by indirect ELISA. On day 12, all IC groups exhibited significantly higher IgY levels compared to the UC and UU groups ($P < 0.0001$). Among the IC groups, the rEnGPX-200 μg group elicited the strongest antibody response, followed by the 100 μg and 50 μg groups, with significant differences observed among all IC groups ($P < 0.001$) (Fig. 1F(a)). By day 19, IgY levels further increased in all IC groups. The rEnGPX-200 μg group maintained the highest IgY

Table 3
Protective efficacy of rEnGPX vaccination on *E. necatrix* challenge.

Groups	Body weight gains (g)	Relative weight gain (%)	lesion scores	oocyst reduction (%)	Sporulation reduction rate (%)	Anticoccidial index (ACI)
rEnGPX−200 μg	137.17 ± 7.03^{ab}	94.81	1.30 ± 0.23^{b}	45.14	82.67	161.81
rEnGPX−100 μg	122.21 ± 9.07^{ab}	84.47	1.70 ± 0.24^{bc}	54.85	84	157.47
rEnGPX−50 μg	131.92 ± 9.64^{ab}	91.18	1.55 ± 0.27^{bc}	21.90	87.33	135.68
UC	114.62 ± 11.84^{a}	79.22	2.20 ± 0.24^{c}	0.00	95.33	117.22
UU	144.68 ± 4.24^{b}	100.00	0.00 ± 0.00^{a}	0	-	200

Note: a–d values with different letters in the same column are significantly different ($P < 0.05$) according to the ANOVA Duncan test.

concentration, which was significantly higher than that of the rEnGPX-100 μg group ($P < 0.0001$). The UC and UU groups remained at baseline levels, with IgY concentrations significantly lower than those of all IC groups ($P < 0.0001$) (Fig. 1F(b)).

4. Discussion

In this study, we identified and functionally characterized a novel glutathione peroxidase, EnGPX, from *E. necatrix*, which is implicated in oocyst wall formation and modulation of host immune responses. The development of the oocyst wall represents a pivotal stage in the life cycle of *Eimeria* spp., serving as a structurally robust and functionally vital barrier. This wall confers substantial mechanical strength and environmental resilience, thereby facilitating parasite survival and efficient transmission (Mai et al., 2009). The biogenesis of the oocyst wall is initiated during gametogenesis, during which two types of WFBs (WFBI and WFBII) in macrogametocytes provide essential structural precursors and key enzymes to the developing wall. Among them, WFBII is particularly enriched in tyrosine-rich glycoproteins and redox enzymes. These components are sequentially discharged and assembled into a highly ordered reticulated bilayer structure, which forms the mature oocyst wall (Belli et al., 2003; Sharman, 2013). The construction of this complex architecture relies not only on the precise assembly of structural proteins, but also on the coordinated action of multiple redox-regulatory enzymes, which collectively contribute to the stable crosslinking of wall-associated proteins (Sharman, 2013; Wang et al., 2023b).

GPXs constitute a widely conserved family of antioxidant enzymes present across animals, plants, and protozoa (Brigelius-Flohé and Maiorino, 2013). Their primary function is to catalyze the reduction of hydrogen peroxide and organic hydroperoxides into non-toxic molecules, utilizing GSH as an electron donor. Through this activity, GPXs effectively scavenge reactive oxygen species (ROS) and play a pivotal role in maintaining intracellular redox homeostasis (Pei et al., 2023). Classical GPXs typically utilize a selenocysteine (Sec) residue at their active site, which confers exceptional catalytic efficiency(Handy et al., 2021). In contrast, the EnGPX characterized in this study belongs to the Cys-GPX subfamily, in which the active-site Sec is replaced by a cysteine residue. This substitution likely underlies altered catalytic kinetics and substrate preference, consistent with the evolutionary shift in non-mammalian GPXs toward thioredoxin-based electron transfer (Flohé and Brigelius-Flohé, 2011). Although the catalytic efficiency of Cys-GPXs is generally lower than that of their Sec-containing counterparts, they can still effectively reduce hydrogen peroxide and organic hydroperoxides, thereby maintaining cellular redox homeostasis (Flohé and Brigelius-Flohé, 2011). Most non-mammalian GPX enzymes have undergone an evolutionary replacement of Sec with Cys and preferentially utilize thioredoxin rather than glutathione (GSH) as the electron donor, highlighting their specialized role in oxidative stress defense (Flohé and Brigelius-Flohé, 2011; Trenz et al., 2021; Maiorino et al., 2007). Such biochemical specialization is thought to provide adaptive advantages under developmentally regulated oxidative stress conditions, including those encountered by parasitic organisms during intracellular differentiation or cyst formation (Guevara-Flores et al., 2024; Pawłowska et al., 2023).

The CxxC motif is a hallmark catalytic signature of thioredoxin-fold oxidoreductases, mediating disulfide bond formation, isomerization, and reduction (Pedone et al., 2010; Wang et al., 2023). Among its variants, the CxxT motif, characterized by substitution of the terminal cysteine in CxxC with threonine, has garnered increasing attention (Fomenko and Gladyshev, 2003). This subtle substitution reshapes the active-site microenvironment, stabilizes the catalytic thiolate via a hydrogen-bond network, and facilitates efficient peroxide reduction with potential thioredoxin preference (Fomenko and Gladyshev, 2003; Pei et al., 2023). In this study, we identified EnGPX as a typical CxxT-motif enzyme. Distinct from classical GPXs, EnGPX lacks the conserved CxxC motif, and its active-site features indicate a possible dependence on noncanonical electron donors, such as thioredoxin, to complete the catalytic cycle. This trait aligns with the evolutionary trend of cysteine substituting for selenocysteine in the GPX systems of parasites, suggesting that the CxxT motif of EnGPX represents a specialized adaptation to oxidative stress defense (Pawłowska et al., 2023; Trenz et al., 2021). Such an adaptation is likely critical for parasite survival within the highly oxidative milieu of host cells (Huang et al., 2012).

The localization and expression profile of EnGPX within the parasite provide compelling evidence for its functional involvement in oocyst wall formation. Immunofluorescence analysis revealed that EnGPX is specifically localized to the WFBII of gametocytes and is progressively incorporated into the developing oocyst wall, suggesting that it directly participates in the cross-linking and stabilization of wall proteins. Consistently, transcriptional analysis showed that E*ngpx* expression peaks at the unsporulated oocyst stage, indicating a role not only in initial wall assembly but also in oocyst maturation and sporulation. Notably, Western blot analysis demonstrated that the native EnGPX protein migrates at approximately 35 kDa, higher than its predicted mass of 27.7 kDa, which likely reflects post-translational modification or conformational effects on mobility.

The immunological relevance of EnGPX is not limited to its enzymatic function. Immunization with rEnGPX elicited an effective humoral response in chickens, which was associated with reduced oocyst shedding, decreased lesion severity, and lower sporulation rates following *E. necatrix* challenge. ACI analysis further revealed that the rEnGPX-200 μg group exhibited the highest ACI value (161.81), indicating moderate protective efficacy. However, these findings are preliminary and require further validation through additional experimental studies to assess their robustness and reproducibility. The mitigation of clinical symptoms and parasite replication indicates that the host immune system recognizes rEnGPX as a key molecule during parasite development, effectively limiting transmission. In contrast to conventional surface or metabolic antigens, targeting an enzyme essential for oocyst wall biogenesis allows stage-specific disruption of the parasite life cycle, highlighting rEnGPX as a promising immunoprophylactic candidate in poultry. However, the noncanonical CxxT motif raises key mechanistic questions regarding its electron donor usage and redox cycle. Future work integrating X-ray crystallography, cryo-EM, and site-directed mutagenesis will be essential to define its catalytic mechanism and donor specificity.

In summary, EnGPX emerges as a critical redox enzyme that contributes to the structural integrity of the *E. necatrix* oocyst wall and exhibits significant potential as an immunogenic subunit vaccine candidate. This work establishes a foundation for understanding apicomplexan redox regulation and informs the development of targeted coccidiosis control strategies.

CRediT authorship contribution statement

Zhuang Ye: Investigation. **Yuemei Peng:** Investigation. **Feiyan Wang:** Writing – original draft, Investigation. **Dandan Liu:** Writing – review & editing, Funding acquisition. **Yu Zhang:** Investigation, Funding acquisition. **Yongcui Feng:** Investigation. **Jianping Tao:** Writing – review & editing, Funding acquisition. **Jinjun Xu:** Writing – review & editing.

Ethical approval

Ethical approval was obtained from the Animal Experiment Ethics Committee of Yangzhou University (Approval No. 202402010) on February 20, 2024.

Mice were anaesthetized by carbon dioxide (CO_2) inhalation prior to retro-orbital blood collection. CO_2 was introduced into the chamber at a gradual displacement rate of 20–30 % of the chamber volume per minute, allowing the animals to gradually lose consciousness and

ensuring that sampling was conducted in a pain-free state.

Chickens were euthanized *via* CO_2 inhalation using a gradual-fill method, in which the CO_2 concentration was steadily increased to 60–70 % of the chamber volume, ensuring a humane and distress-free induction of unconsciousness.

Funding

This work was supported by the National Natural Science Foundation of China (No. 31602039 to LD, No. 31972698 to JT); the Postgraduate Research & Practice Innovation Projects of Jiangsu Province (KYCX25_4076); the 111 Project D18007, the Priority Academic Program Development of Jiangsu Higher Education Institutions (PAPD).

Declaration of Competing Interest

The authors declare that they have no known competing financial interests or personal relationships that could have appeared to influence the work reported in this paper.

Acknowledgement

We truly appreciate the time and effort volunteered by the Associate Prof. Dandan Liu and Yuemei Peng during the hard-working days. We would also like to thank Home for Researchers (www. home-for-researchers. com) and ChatGPT for their assistance with language polishing, which helped to enhance the clarity and fluency of this manuscript.

References

Belli, S.I., Wallach, M.G., Luxford, C., Davies, M.J., Smith, N.C., 2003. Roles of tyrosine-rich precursor glycoproteins and dityrosine- and 3,4-dihydroxyphenylalanine-mediated protein cross-linking in development of the oocyst wall in the coccidian parasite *Eimeria maxima*. Eukaryot. Cell 2, 456–464. https://doi.org/10.1128/EC.2.3.456-464.2003.

Blake, D.P., 2025. *eimeria* of chickens: the changing face of an old foe. Avian Pathol. 112. https://doi.org/10.1080/03079457.2024.2441180.

Brigelius-Flohé, R., Maiorino, M., 2013. Glutathione peroxidases. Biochim. Et. Biophys. Acta (BBA) Gen. Subj. 1830, 3289–3303. https://doi.org/10.1016/j.bbagen.2012.11.020.

Chapman, H.D., 2018. Applied strategies for the control of coccidiosis in poultry. CABI Rev. 1–11. https://doi.org/10.1079/PAVSNNR201813026.

Chapman, H.D., Rathinam, T., 2022. Focused review: the role of drug combinations for the control of coccidiosis in commercially reared chickens. Int. J. Parasitology Drugs Drug Resistance 18, 32–42. https://doi.org/10.1016/j.ijpddr.2022.01.001.

Chen, Y.-I., Wei, P.-C., Hsu, J.-L., Su, F.-Y., Lee, W.-H., 2016. NPGPx (GPx7): a novel oxidative stress sensor/transmitter with multiple roles in redox homeostasis. Am. J. Transl. Res 8, 1626–1640.

Ferguson, D.J.P., Belli, S.I., Smith, N.C., Wallach, M.G., 2003. The development of the macrogamete and oocyst wall in *eimeria maxima*: immuno-light and electron microscopy. Int J. Parasitol. 33, 1329–1340. https://doi.org/10.1016/s0020-7519(03)00185-1.

Flohé, L., Brigelius-Flohé, R., 2011. Selenoproteins of the glutathione peroxidase family. In: Hatfield, D.L., Berry, M.J., Gladyshev, V.N. (Eds.), Selenium. Springer New York, New York, NY, pp. 167–180. https://doi.org/10.1007/978-1-4614-1025-6_13.

Flohé, L., Toppo, S., Orian, L., 2022. The glutathione peroxidase family: discoveries and mechanism. Free Radic. Biol. Med. 187, 113–122. https://doi.org/10.1016/j.freeradbiomed.2022.05.003.

Fomenko, D.E., Gladyshev, V.N., 2003. Identity and functions of CxxC-Derived motifs. Biochemistry 42, 11214–11225. https://doi.org/10.1021/bi034459s.

Guevara-Flores, A., Nava-Balderas, G., De Jesús Martínez-González, J., Vásquez-Lima, C., Rendón, J.L., Del Arenal Mena, I.P., 2024. A physiological approach to explore how Thioredoxin–Glutathione reductase (TGR) and peroxiredoxin (Prx) eliminate H2O2 in cysticerci of taenia. Antioxidants 13, 444. https://doi.org/10.3390/antiox13040444.

Handy, D.E., Joseph, J., Loscalzo, J., 2021. Selenium, a micronutrient that modulates cardiovascular health via redox enzymology. Nutrients 13, 3238. https://doi.org/10.3390/nu13093238.

Huang, H.-H., Rigouin, C., Williams, D.L., 2012. The redox biology of schistosome parasites and applications for drug development. Curr. Pharm. Des. 18, 3595–3611.

Johnson, J., Reid, W.M., 1970. Anticoccidial drugs: lesion scoring techniques in battery and floor-pen experiments with chickens. Exp. Parasitol. 28, 30–36. https://doi.org/10.1016/0014-4894(70)90063-9.

Liu, D., Cao, L., Zhu, Y., Deng, C., Su, S., Xu, J., Jin, W., Li, J., Wu, L., Tao, J., 2014. Cloning and characterization of an *eimeria necatrix* gene encoding a gametocyte protein and associated with oocyst wall formation. Parasites Vectors 7, 27. https://doi.org/10.1186/1756-3305-7-27.

Livak, K.J., Schmittgen, T.D., 2001. Analysis of relative gene expression data using Real-Time quantitative PCR and the $2^{-\Delta\Delta CT}$ method. Methods 25, 402–408. https://doi.org/10.1006/meth.2001.1262.

Mai, K., Sharman, P.A., Walker, R.A., Katrib, M., De Souza, D., McConville, M.J., Wallach, M.G., Belli, S.I., Ferguson, D.J.P., Smith, N.C., 2009. Oocyst wall formation and composition in coccidian parasites. Mem. Inst. Oswaldo Cruz 104, 281–289. https://doi.org/10.1590/s0074-02762009000200022.

Mai, K., Smith, N.C., Feng, Z.-P., Katrib, M., Šlapeta, J., Šlapetova, I., Wallach, M.G., Luxford, C., Davies, M.J., Zhang, X., Norton, R.S., Belli, S.I., 2011. Peroxidase catalysed cross-linking of an intrinsically unstructured protein via dityrosine bonds in the oocyst wall of the apicomplexan parasite, *Eimeria maxima*. Int. J. Parasitol. 41, 1157–1164. https://doi.org/10.1016/j.ijpara.2011.07.001.

Maiorino, M., Ursini, F., Bosello, V., Toppo, S., Tosatto, S.C.E., Mauri, P., Becker, K., Roveri, A., Bulato, C., Benazzi, L., De Palma, A., Flohé, L., 2007. The thioredoxin specificity of drosophila GPx: a paradigm for a Peroxiredoxin-like mechanism of many glutathione peroxidases. J. Mol. Biol. 365, 1033–1046. https://doi.org/10.1016/j.jmb.2006.10.033.

McManus, E.C., Campbell, W.C., Cuckler, A.C., 1968. Development of resistance to quinoline coccidiostats under field and laboratory conditions. J. Parasitol. 54, 1190–1193.

Pawłowska, M., Mila-Kierzenkowska, C., Szczegielniak, J., Woźniak, A., 2023. Oxidative stress in parasitic Diseases-Reactive oxygen species as mediators of interactions between the host and the parasites. Antioxidants 13, 38. https://doi.org/10.3390/antiox13010038.

Pedone, E., Limauro, D., D'Ambrosio, K., De Simone, G., Bartolucci, S., 2010. Multiple catalytically active thioredoxin folds: a winning strategy for many functions. Cell. Mol. Life Sci. 67, 3797–3814. https://doi.org/10.1007/s00018-010-0449-9.

Peek, H.W., Landman, W.J.M., 2011. Coccidiosis in poultry: anticoccidial products, vaccines and other prevention strategies. Vet. Q. 31, 143–161. https://doi.org/10.1080/01652176.2011.605247.

Pei, J., Pan, X., Wei, G., Hua, Y., 2023. Research progress of glutathione peroxidase family (GPX) in redoxidation. Front. Pharm. 14, 1147414. https://doi.org/10.3389/fphar.2023.1147414.

Pittilo, R.M., Ball, S.J., 1980. The ultrastructural development of the oocyst wall of *Eimeria maxima*. Parasitology 81, 115–122. https://doi.org/10.1017/s0031182000055086.

Sharman, P.A., 2013. Identification of Enzymes Potentially Involved in the Formation of the Oocyst Wall of Coccidian Parasites. James Cook University. https://doi.org/10.25903/28SX-BH70.

Su, S., Hou, Z., Liu, D., Jia, C., Wang, L., Xu, J., Tao, J., 2017. Comparative transcriptome analysis of second- and third-generation merozoites of *eimeria necatrix*. Parasit. Vectors 10, 388. https://doi.org/10.1186/s13071-017-2325-z.

Trenz, T.S., Delaix, C.L., Turchetto-Zolet, A.C., Zamocky, M., Lazzarotto, F., Margis-Pinheiro, M., 2021. Going forward and back: the complex evolutionary history of the GPx. Biology 10, 1165. https://doi.org/10.3390/biology10111165.

Venkatas, J., Adeleke, M.A., 2019. A review of Eimeria antigen identification for the development of novel anticoccidial vaccines. Parasitol. Res 118, 1701–1710. https://doi.org/10.1007/s00436-019-06338-2.

Wallach, M., Smith, N.C., Petracca, M., Miller, C.M., Eckert, J., Braun, R., 1995. *Eimeria maxima* gametocyte antigens: potential use in a subunit maternal vaccine against coccidiosis in chickens. Vaccine 13, 347–354. https://doi.org/10.1016/0264-410x(95)98255-9.

Wang, J., Chitsaz, F., Derbyshire, M.K., Gonzales, N.R., Gwadz, M., Lu, S., Marchler, G. H., Song, J.S., Thanki, N., Yamashita, R.A., Yang, M., Zhang, D., Zheng, C., Lanczycki, C.J., Marchler-Bauer, A., 2023. The conserved domain database in 2023. Nucleic Acids Res. 51, D384–D388. https://doi.org/10.1093/nar/gkac1096.

Wang, L., Liu, D., Gao, Y., Hou, Z., Zhu, Y., Wang, F., Li, W., Zhang, A., Xu, J., Hu, J., Tao, J., 2023a. Examination of gametocyte protein 22 localization and oocyst wall formation in *Eimeria necatrix* using laser confocal microscopy and scanning electron microscopy. Parasites Vectors 16, 124. https://doi.org/10.1186/s13071-023-05742-z.

Wang, L., Liu, D., Zhu, Y., Wang, F., Cai, W., Feng, Q., Su, S., Hou, Z., Xu, J., Hu, J., Tao, J., 2023b. Comparative proteomic analysis of wall-forming bodies and oocyst wall reveals the molecular basis underlying oocyst wall formation in *Eimeria necatrix*. Parasit. Vectors 16, 460. https://doi.org/10.1186/s13071-023-06076-6.

Xu, L., Li, X., 2024. Conserved proteins of *Eimeria* and their applications to develop universal subunit vaccine against chicken coccidiosis. Vet. Vaccin. 3, 100068. https://doi.org/10.1016/j.vetvac.2024.100068.